Complex absorbing potential and Chebyshev propagation scheme

S. Midgley and J. B. Wang
Department of Physics, The University of Western Australia, Perth 6907, Australia
(Received 9 February 1999; revised manuscript received 8 July 1999)

This work presents a detailed analysis of complex absorbing potentials employed to eliminate reflection or wrap-around of wave packets at numerical grid boundaries. In particular, a limiting value for the maximum propagation time step is derived, beyond which the complex potential may introduce massive errors and the Chebyshev propagation scheme is found to fail.

PACS number(s): 02.70.−c, 73.23.Ad, 73.23.Hk

I. INTRODUCTION

Numerically solving the time-dependent Schrödinger equation often requires large numerical grids to represent the system Hamiltonian and the dynamics of its wave function. This can be prohibitively expensive in terms of computer memory and computational time. Recent advances are focused on developing computation techniques to reduce the size of the numerical grid to include only the interaction region. One of the ideas is to remove those components of the wave function which have left the interaction region and are going to propagate further as free waves. By doing so one can explore the time evolution of the slower components of the wave function still under the influence of the interaction potentials, without the complication arising from the reflection or wrap-around of the faster components at the grid boundaries.

Methods used to remove the fast components of the wave function outside the interaction region have varied from using lines of no return, complex optical potentials in the Hamiltonian, and the split operator Hamiltonian [1]. The most attractive of these is the complex absorbing potential, which absorbs the wave-function components just before they reach the grid boundaries [2]. The complex potential is easy to implement, requires little extra computation power, and has been found to be very effective at absorbing the wave packet [3].

The main drawback of the complex potential is that the final wave function cannot be reconstructed. In other words, the absorbed components are effectively lost. It also produces artificial reflections, however these can be minimized due to the freedom in the design of complex potentials. Various schemes have been proposed, which vary the shape of the absorbing potential and adjust the slope and depth to reduce reflection while maximizing the absorption [4–7]. These analyses, however, have been carried out only for propagation schemes using short time steps. We found that the complex potential introduces massive errors when naively implemented in the Chebyshev propagation scheme [8,9], where arbitrarily large time steps can be used. The main problem is the lack of understanding of how the time step used in the propagation affects the result. Since most previous work with complex potentials involved small time steps, this problem was not present. It was pointed out by Vibok and Balint-Kurt [4] that the complex potential must act adiabatically, which implies that it must not change by a large amount in any single time step. This is clearly not the case for the Chebyshev propagation scheme.

The outline of the paper is as follows. Section II presents an analysis of how the complex potential absorbs the wave function and why the time step is a critical factor in assuring this ability. A maximum time step $t_{\max}$ is established, beyond which the Chebyshev propagation scheme with the complex potential is found to fail. Section III provides numerical evidence that, using a time step less than $t_{\max}$, the complex potential works well with the Chebyshev propagation scheme.

II. THEORY

The general Schrödinger equation is

$$\imath \frac{\partial \psi(\mathbf{r},t)}{\partial t} = \mathcal{H}\psi(\mathbf{r},t) \tag{1}$$

with solution

$$\psi(\mathbf{r},t) = \exp(-\imath \mathcal{H} t)\,\psi(\mathbf{r},0), \tag{2}$$

where the system Hamiltonian $\mathcal{H} = -(1/2m)\nabla^2 + \mathcal{V}(\mathbf{r})$, $\mathcal{V}(\mathbf{r})$ is the interaction potential, and m is the effective mass of the system. Atomic units are used in this paper.

The Chebyshev scheme approximates the exponential time propagator by a Chebyshev polynomial expansion [8]

$$\psi(\mathbf{r},t) = \exp[-\imath(\mathcal{E}_{\max}+\mathcal{E}_{\min})t] \sum_{n=0}^{\mathcal{N}} a_n(\alpha)\,\phi_n(-\imath\tilde{\mathcal{H}})\,\psi(\mathbf{r},0), \tag{3}$$

where $\mathcal{E}_{\min}$ and $\mathcal{E}_{\max}$ are the minimum and maximum energy eigenvalues, $a_n(\alpha) = 2J_n(\alpha)$ except for $a_0(\alpha) = J_0(\alpha)$, $J_n(\alpha)$ are the Bessel functions of the first kind, ϕ_n are the Chebyshev polynomials, and the normalized Hamiltonian is defined as

$$\tilde{\mathcal{H}} = \frac{1}{\mathcal{E}_{\max}-\mathcal{E}_{\min}}[2\mathcal{H} - \mathcal{E}_{\max} - \mathcal{E}_{\min}]. \tag{4}$$

This propagation scheme propagates the wave function $\psi(\mathbf{r},t)$ for any time step t, and it is often referred to as a long time propagator.

The introduction of a complex potential modifies the Schrödinger equation

$$\imath\frac{\partial\psi(\mathbf{r},t)}{\partial t}=(\mathcal{H}-\imath\mathcal{U})\psi(\mathbf{r},t) \tag{5}$$

and the solution

$$\psi(\mathbf{r},t)=\exp(-\imath\mathcal{H}t-\mathcal{U}t)\psi(\mathbf{r},0). \tag{6}$$

This is no longer a true Schrödinger equation, but if applied correctly, the complex potential $\mathcal{U}$ only absorbs the wave function incident on it without affecting the wave function at other regions. Following is a discussion of how the complex potential works and then a limit is established for the maximum workable time step.

Using the *Baker-Campbell-Hausdorff* formula [10]

$$\exp(A+B)=\exp(A)\exp(B)\times\exp\left(-\frac{1}{2}[A,B]+\frac{1}{6}[A,[A,B]]-\frac{1}{3}[B,[B,A]]+\cdots\right), \tag{7}$$

one can expand Eq. (6) as

$$\psi(\mathbf{r},t)=\exp(-\imath\mathcal{H}t)\exp(-\mathcal{U}t)\times\exp\left(-\imath\frac{1}{2}[\mathcal{H},\mathcal{U}]t^2+\frac{1}{6}[\mathcal{H},[\mathcal{H},\mathcal{U}]]t^3+\frac{\imath}{3}[\mathcal{U},[\mathcal{U},\mathcal{H}]]t^3\cdots\right)\psi(\mathbf{r},0). \tag{8}$$

Since the interaction potential $\mathcal{V}$ and the complex absorbing potential $\mathcal{U}$ are defined nonzero in different regions, they can be considered separately. Now consider the noninteraction region where the complex potential $\mathcal{U}$ is nonzero while $\mathcal{V}=0$. We have

$$\psi(\mathbf{r},t)=\exp(-\imath\mathcal{H}t)\exp(-\mathcal{U}t)\times\exp\left(-\imath\frac{1}{4m}[\nabla^2,\mathcal{U}]t^2+\frac{1}{24m^2}[\nabla^2,[\nabla^2,\mathcal{U}]]t^3+\frac{\imath}{6m}[\mathcal{U},[\mathcal{U},\nabla^2]]t^3\cdots\right)\psi(\mathbf{r},0). \tag{9}$$

For convenience, the following analysis is carried out using a linear ramp in the x direction as the complex potential defined by

$$\mathcal{U}(x,y)=\begin{cases}ax+b, & x>-b\\ 0 & \text{otherwise,}\end{cases} \tag{10}$$

where b is the starting point and a is the slope of the complex potential. In this case the commutator relations in Eq. (9) are, for any arbitrary function ψ,

$$[\nabla^2,x]\psi=2\partial_x\psi, \tag{11}$$

$$[x,[x,\nabla^2]]\psi=-2[x,\partial_x]\psi=2\psi, \tag{12}$$

$$[\nabla^2,[\nabla^2,x]]\psi=2[\nabla^2,\partial_x]\psi=0. \tag{13}$$

The higher-order commutators in the expansion are zero as only constants, which commute with each other, are present. Equation 9 then becomes

$$\psi(\mathbf{r},t)=\exp(-\imath\mathcal{H}t)\exp[-(ax+b)t]\times\exp\left(-\imath\frac{a}{2m}\partial_x t^2+\imath\frac{a^2}{3m}t^3\right)\psi(\mathbf{r},0). \tag{14}$$

Note that $\exp(-\imath(a/2m)\partial_x t^2)$ is exactly the Taylor expansion of $\psi(x-\imath(a/2m)t^2,y,z,0)$, so

$$\psi(\mathbf{r},t)=\exp(-\imath\mathcal{H}t)\exp[-(ax+b)t]\times\exp\left(\imath\frac{a^2}{3m}t^3\right)\psi\left(x-\imath\frac{a}{2m}t^2,y,z,0\right). \tag{15}$$

From the above solution, it is clear that the wave function $\psi(\mathbf{r},t)$ can blow up rapidly if the time step t is too big. However, if t is chosen such that

$$\left\|\exp\left(\imath\frac{a^2}{3m}t^3\right)\psi\left(x-\imath\frac{a}{2m}t^2,y,z,0\right)\right\|\leqslant 1 \tag{16}$$

over the range of the complex potential, the complex potential would reduce exponentially the magnitude of the wave packet across the complex potential. For simplicity, only the x dimension was considered, since the other dimensions can be included trivially. Assuming that the initial wave function is a Gaussian, i.e., $\psi(x,0)=(1/\sqrt{2\pi}w)\exp\{[-(x-x_0)^2/2w^2]+\imath p_x(x-x_0)\}$, then

$$\begin{aligned}&\left\|\exp\left(\imath\frac{a^2}{3m}t^3\right)\psi\left(x-\imath\frac{a}{2m}t^2,0\right)\right\|\\&=\frac{1}{\sqrt{2\pi}w}\left\|\exp\left[-2\left(\frac{x-\imath\frac{a}{2m}t^2-x_0}{2w}\right)^2+\imath p_x\left(x-\imath\frac{a}{2m}t^2-x_0\right)\right]\right\|\\&=\frac{1}{\sqrt{2\pi}w}\exp\left[-2\left(\frac{x-x_0}{2w}\right)^2+\frac{2}{(2w)^2}\frac{a^2}{4m^2}t^4+p_x\frac{a}{2m}t^2\right].\end{aligned} \tag{17}$$

Because the time t cannot be complex or negative, the only viable solution to the inequality Eq. (16) is

$$t\leqslant\sqrt{\frac{2m}{a}[\sqrt{p_x^2w^4+2\ln(\sqrt{2\pi}w)w^2+(x-x_0)^2}-p_xw^2]}, \tag{18}$$

which sets a limiting value for the maximum time step. If multiple time steps are required to complete a calculation, $\psi(x,0)$ would be the wave packet of the previous time step and will generally not be a Gaussian. In other words, its momentum will not be localized around p_x and its position expectation value will not be x_0. To overcome this, the above limit on t can be tightened by (i) substituting $p_{\max}$ for p_x,

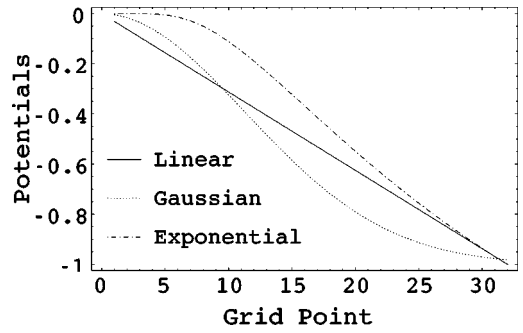

FIG. 1. Complex potentials used in calculations.

where $p_{\max}$ is the maximum momentum that the numerical grid can support, and (ii) assuming that the wave packet has already reached the complex potential, i.e., $x=x_0$. This provides the smallest limit for t, i.e.,

$$t \leqslant \sqrt{\frac{2m}{a}\left[\sqrt{p_{\max}^2 w^4 + 2\ln(\sqrt{2\pi}w)w^2} - p_{\max} w^2\right]}, \tag{19}$$

that should then work for all cases.

Although this criterion is derived using the linear complex potential given by Eq. (10), it is found to be applicable to other types of potentials as well, for example, a Gaussian edge and an exponential potential given by

$$\imath\mathcal{U}_0\left[\exp\left(-\frac{2(x-b)^2}{a^2}\right)-1\right] \tag{20}$$

and

$$-\imath\mathcal{U}_0\exp\left(1-\frac{a}{(x-b)^2}\right), \tag{21}$$

where $\mathcal{U}_0$ and a define the height and the width of the complex potential, and b is where the potential starts. Figure 1 shows the three potentials.

As expected, the maximum time given by Eq. (18) is dependent on the distance from the complex potential to the initial position of the wave packet. If the complex potential was at infinity, it would have no effect on the local propagation of the wave packet and would then allow arbitrarily long time steps as predicted by Eq. (18). Note that the maximum time step is not zero even when the wave packet is at the complex potential. This is attractive from a computation point of view, which means that there is always some finite time step that will produce the results required.

According to Child [2], the depth $\mathcal{U}_0$ and the width Δr of the linear ramp complex potential should satisfy the following simple relation:

$$\frac{\hbar E}{\Delta r\sqrt{8m}} \ll \mathcal{U}_0 \ll \frac{\Delta r\sqrt{8m}E^{3/2}}{\hbar}, \tag{22}$$

where E is the translation energy and m is the mass. The slope of the complex potential is given by $a=\mathcal{U}_0/\Delta r$. The starting point for the complex potential is normally very close to the boundary. The choice of $\mathcal{U}_0$ can be made such that

$$\beta\frac{\hbar E}{\Delta r\sqrt{8m}} = \mathcal{U}_0 = \frac{1}{\beta}\frac{\Delta r\sqrt{8m}E^{3/2}}{\hbar} \tag{23}$$

provided

$$\beta = \frac{\Delta r\sqrt{8m}E^{1/4}}{\hbar} \ll 1. \tag{24}$$

Elimination of β gives

$$\mathcal{U}_0 = E^{5/4}. \tag{25}$$

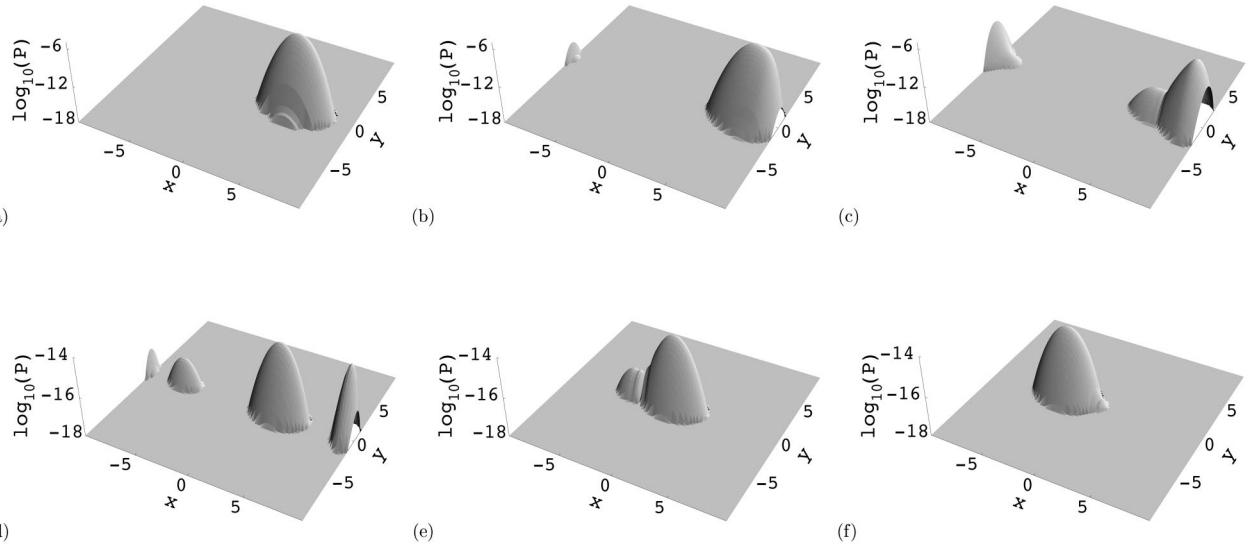

FIG. 2. Propagation of an electron wave packet in free space with the exponential complex potential at the right end of the grid. The probability function $P(t)=\psi^*(x,y,t)\psi(x,y,t)$ is plotted in logarithm scale. Flow of time t is left to right and top to bottom with time step satisfying Eq. (18). The spatial units (x and y axes) are $\times 1000$ a.u.

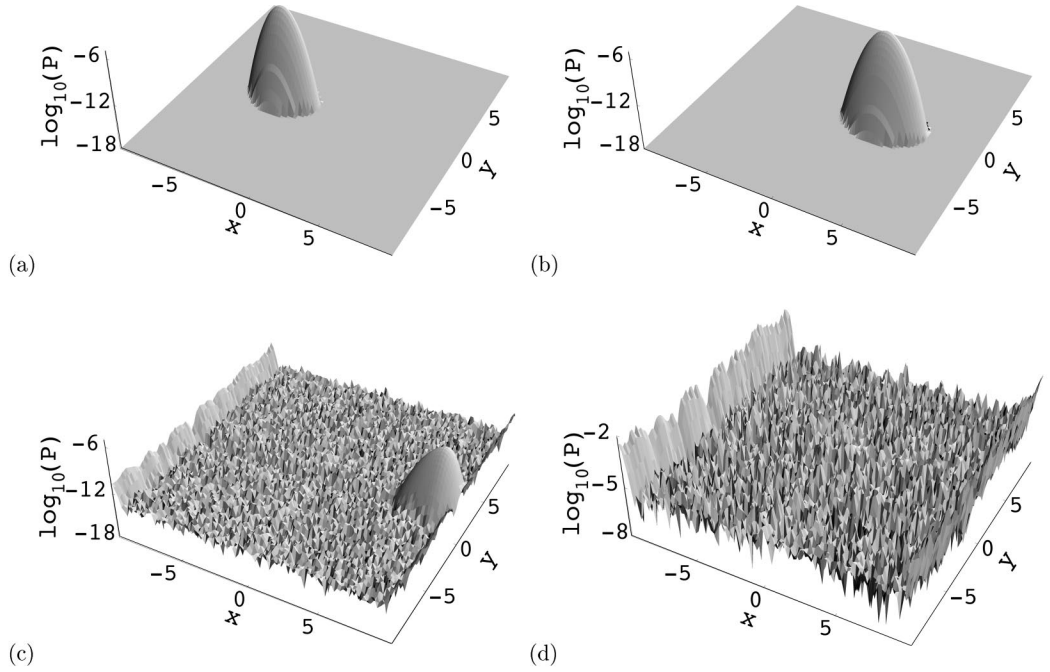

FIG. 3. Massive errors are introduced by the complex potential when Eq. (18) no longer holds (same units as Fig. 2).

This is convenient as $\mathcal{U}_0$ is independent of the width of the complex potential Δr, as long as Eq. (24) is satisfied.

III. RESULTS AND DISCUSSIONS

As an example of implementing the complex absorbing potential in the Chebyshev scheme, we first consider an electron wave packet propagating in free space with the exponential complex potential given by Eq. (21). In this case x_0 and p_x of the wave packet are well defined at all times and thus we can determine a maximum time step by using Eq. (18), instead of the tighter limit set by Eq. (19). The propagation of the electron is shown in Fig. 2. The initial energy of the wave packet is arbitrarily chosen as 0.0300 a.u. The effective mass is taken as 0.0667 a.u. for GaAs. The numerical grid in use is found to support a maximum momentum of $p_{\max}=0.0895$ a.u. The propagation of the wave packet is divided into nine equally spaced time steps with $t_{\text{step}}=42.5$ fs, which satisfies the criterion given by Eq. (18).

Figures 2(a)–2(c) shows the wave packet approaching the edge of the grid space and gradually spreading as it travels. When it hits the boundary, the wave packet is absorbed by the complex potential and only a slight reflected wave packet is observed [see Figs. 2(d)–2(f)]. The magnitude of the wave packet before the edge of the space and the reflected wave packet are about 10^{-6} and 10^{-15}, respectively. The reflected wave packet can introduce error into further calculations when it starts to interact with the slower components of the wave packet still in the interaction region. However, since the reflected wave packet is about 10^9 times smaller than the incident wave packet, this effect is very small.

Despite the small reflection and high accuracy of the method, we found that the Chebyshev expansion scheme is very sensitive to the presence of a complex potential. A small change in the time step for each propagation gave rise to very different results as illustrated in Fig. 3. In this calculation, the propagation of the wave packet was divided into eight equally spaced time steps with $t_{\text{step}}=47.8$ fs, which no longer satisfies Eq. (18). As shown, large errors are introduced by the complex potential placed at the right end of the numerical grid. It is interesting to note that the wave packet appears to propagate with little error in the first few time steps, even when Eq. (18) is not held. It is not until the wave packet approaches the complex potential that large errors start to enter the calculations. This is supported by the

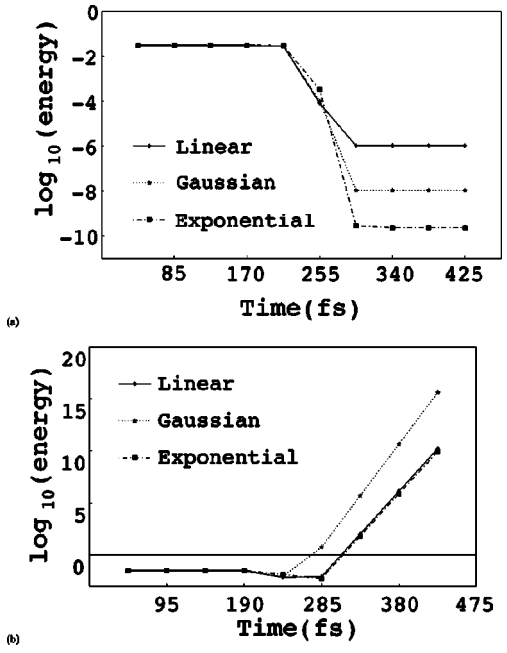

FIG. 4. (a) Absorption of system energy (a.u.) when Eq. (18) is satisfied; (b) energy (a.u.) diverges otherwise.

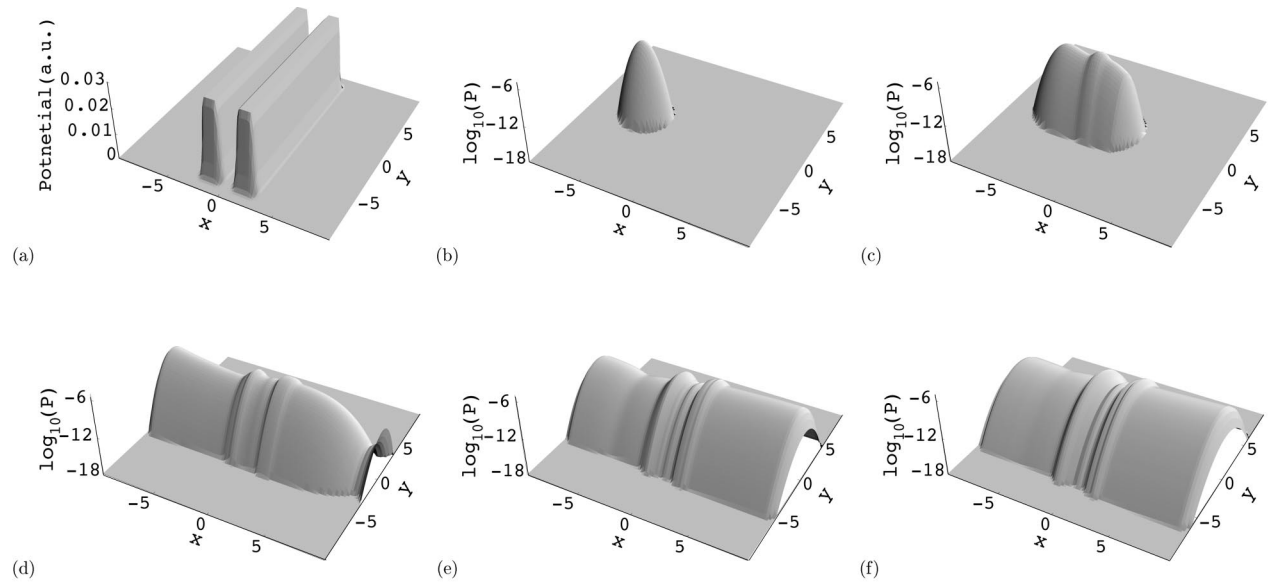

FIG. 5. Propagation of an electron wave packet under the influence of a double barrier with exponential complex potentials at both ends of the grid. Flow of time is left to right and top to bottom with time step satisfying Eq. (19) (same units as Fig. 2).

dependence of Eq. (18) on $x-x_0$.

Figure 4(a) illustrates how well the system energy $E_{\text{system}}=\int \psi^{\star}(\boldsymbol{r},t)\mathcal{H}\psi(\boldsymbol{r},t)d\boldsymbol{r}$ is absorbed by the complex potentials when Eq. (18) holds. For the first five time steps, the system energy is conserved. Then over the following three time steps the majority of the energy is absorbed by the complex potential, leaving only the energy of the reflected wave packet. For the linear, Gaussian, and exponential potentials, the energy of the reflected wave packet is, respectively, about 10^{-6}, 10^{-8}, and 10^{-10} times smaller than the initial system energy. This is very close to complete absorption. Among the three complex potentials, the exponential potential given by Eq. (21) appears to cause the least reflection, which is in agreement with Vibók and Balint-Kurti [4]. However, for all three forms of complex potential, the system energy diverges when the time step was changed from 42.5 fs to 47.8 fs, as shown in Fig. 4(b). This corresponds to the large errors introduced to the wave packet by the complex potential as shown in Fig. 3. Alternatively, we could plot the norm of the wave function as a function of time to show the absorption of flux by complex potentials. Almost identical behavior was observed to that shown in Fig. 4.

Figure 5 illustrates the propagation of an electron wave packet under the influence of a double barrier with complex potentials at both ends of the numerical grid. In this case a smaller grid spacing was adopted which supports a higher maximum momentum $p_{\max}=0.171$ a.u. Also, since x_0 and p_x of the wave packet are not well defined under the influence of the barrier potential, the tighter limit set by Eq. (19) was used, $t_{\max}=26.5$ fs. As shown in Fig. 5, the reflection due to

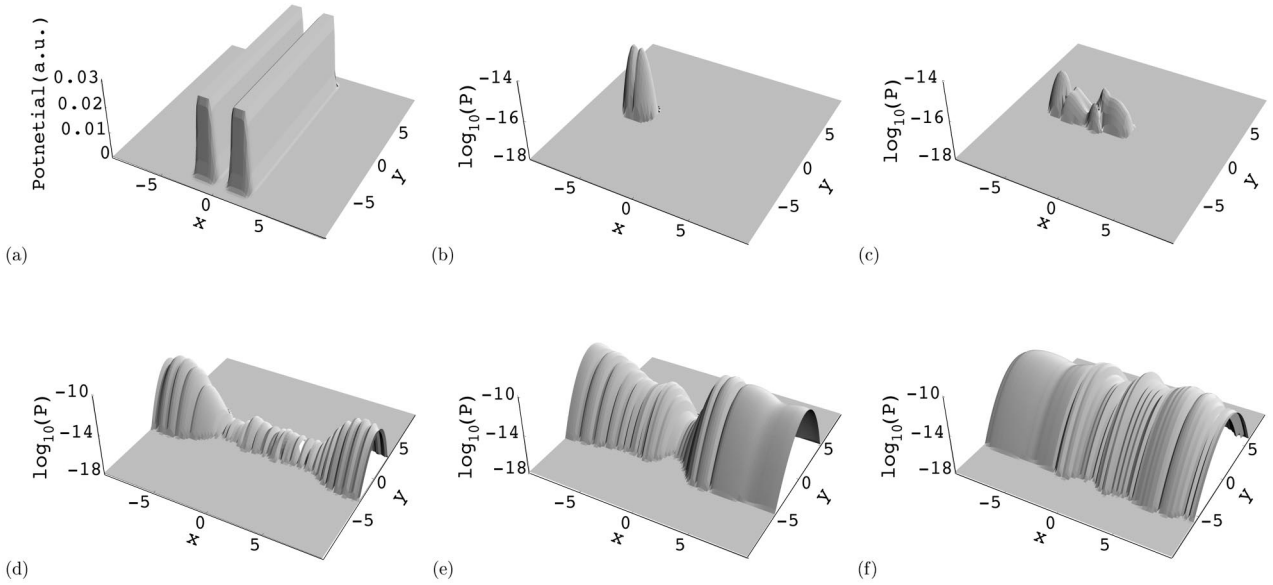

FIG. 6. Absolute errors between the results shown in Fig. 5 and the results obtained without the complex potentials but using a larger numerical grid (same units as Fig. 2).

the complex potential does not visibly affect the wave-packet propagation in the interaction region.

To quantify the errors introduced by the complex potentials, results shown in Fig. 5 were compared with that obtained using a much larger numerical grid but without the complex potentials. The absolute errors are plotted in Fig. 6. As shown, until the wave packet reaches the complex potential, the absolute errors are typically below 10^{-15} (the magnitude of the norm was typically 10^{-6}, resulting in an approximately relative error of 10^{-9}), indicating that the complex boundary does not introduce significant error into the propagation. Once the wave packet reaches the complex potential, a slight reflection occurs giving rise to an error about three orders of magnitude smaller than the slower components of the wave packet still under the influence of the interaction potential.

IV. CONCLUSION

The application of a negative complex potential at the boundary of the numerical grid has been shown to effectively absorb a propagating wave packet. The nature of this absorption is demonstrated along with the possible errors that it can introduce.

Finite difference methods (or other short time propagators), where small time steps are used, do not suffer from large errors introduced by the complex potential. However, this is not the case for long time propagators such as the Chebyshev scheme. The total time propagation may need to be broken up into several smaller pieces to ensure that the time step is less than that given by Eq. (18). Due to the difficulty in evaluating Eq. (18) for each time step, Eq. (19) can be used to provide a global maximum time step.

ACKNOWLEDGMENTS

Calculations were carried out on a 500 MHz Digital Personal Workstation 500 a.u. and a Fujitsu VPP300 Super Computer. The VPP300 Super Computer time was generously donated by the Australian National University Super Computer Facility. We would like to thank Dr. Paul Abbott for discussions associated with analyzing the results in MATHEMATICA and for providing the reference to the *Baker-Campbell-Hausdorff* formula [10].

[1] N. Balakrishnan, C. Kalyanaraman, and N. Sathyamurthy, Phys. Rep. **280**, 79 (1997).
[2] M. Child, Mol. Phys. **72**, 89 (1991).
[3] D. Neuhauser and M. Baer, J. Chem. Phys. **92**, 3419 (1990).
[4] A. Vibók and G. Balint-Kurt, J. Chem. Phys. **96**, 7615 (1992).
[5] D. Macías, S. Brouard, and J. Muga, Chem. Phys. Lett. **228**, 672 (1994).
[6] U. Riss and H.-D. Meyer, J. Phys. B **28**, 1475 (1995).
[7] T. Seideman and W. Miller, J. Chem. Phys. **96**, 4412 (1991).
[8] H. Tal-Ezer and R. Kosloff, J. Chem. Phys. **81**, 3967 (1984).
[9] J. B. Wang and T. Scholz, Phys. Rev. A **57**, 3554 (1998).
[10] J.-M. Normand, *A Lie Group: Rotations in Quantum Mechanics* (North-Holland, Amsterdam, 1980).